Appl Water Sci (2017) 7:3729–3740
DOI 10.1007/s13201-016-0519-8

ORIGINAL ARTICLE

New core@shell nanogel based 2-acrylamido-2-methyl-1-propane sulfonic acid for preconcentration of Pb(II) from various water samples

Kamel Rizq Shoueir[1] · Magda Ali Akl[2] · Ali Ali Sarhan[2] · Ayman Mohamdy Atta[3]

Received: 18 October 2016 / Accepted: 7 December 2016 / Published online: 24 December 2016

Abstract Poly(vinyl alcohol) core coated with poly(2-acrylamido-2-methyl-1-propanesulfonic acid-co-*N*-isopropylacrylamide) shell to produce well-define PVA@-P(AMPS-co-NIPAm) core shell nanogels with a core of 25 ± 0.5 nm and shell of 5 ± 0.5 nm. The synthetic approach was produced by a surfactant free emulsion polymerization (SFEP). The specific area was found to be 1685.8 m^2/g. The nanogels were studied in a batch adsorption for removal of Pb(II) ions and characterized by SEM, TEM, TGA and BET measurements. The results showed that the adsorption equilibrium data fitted the Langmuir isotherm and the kinetic studies are well described by the pseudo-second-order kinetic model. The Pb(II) maximum adsorption was 510.2 (mg/g) for PVA@P(90AMPS-co-10NIPAm) (wt.: wt%). The PVA@P(AMPS-co-NIPAm) nanogels were applied for extracting of Pb(II) in real different environmental water samples successfully with high recoveries reaches 104.4%.

Keywords Nanostructures · Chemical synthesis · Transmission electron microscopy (TEM) · Surface properties

✉ Kamel Rizq Shoueir
kameltag@yahoo.com

[1] Polymer Laboratory, Chemistry Department, Faculty of Science, Mansoura University, Mansoura 35516, Egypt

[2] Chemistry department, Mansoura University, Mansoura, Egypt

[3] Surfactant Research Chair, Chemistry Department, College of Science, King Saud University, Riyadh, Saudi Arabia

Introduction

Many industries have released heavy metals into the environment, including mining, refining, textiles, paints and dyes production (Aguado et al. 2009). Heavy metal ions are toxic, absorbed and accumulated by living organisms. They are non-degradable and highly soluble in the aquatic environments (Ju et al. 2009). The most dangerous contaminants are Pb(II); it can cause severe kidney diseases, nervous disorder and even death (Li et al. 2013). However, Pb(II) is widely used in many important industrial applications, such as the storage battery manufacture, pigment, photographic materials, petrochemicals, printing and fuel combustion (Axtell et al. 2003). Analyte preconcentration technique is a useful sample preparation step in the detection of toxic metals from aqueous samples especially for metals occur at low concentrations (nearly <1 mg/l) in groundwater samples and could pass through many analytical instruments undetected attributed to matrix interference (Liu et al. 2006). Preconcentration used to enhance the recovery of the metals and their determination in different water samples (Darko et al. 2012). In recent decades, various efficient removal techniques have been developed to remove heavy metals, such as solvent extraction, ion exchange, biological degradation and precipitation techniques, but often are costly time-consuming (Khaydarov and Gapurova 2010).

Adsorption an attractive method that allows flexibility in design, ease of operation, capable of the adsorbent to regenerate metal ions by suitable desorbing reagent, highly efficient method for treatment of heavy metals (Rao et al. 2007; Yildi et al. 2010). Adsorbents such as activated carbon, resins and zeolite have been studied; however, their adsorption capacities and time-consuming removal equilibrium are nearly low (Savage and Diallo 2005; Mauter and

Elimelech 2008; Sekar et al. 2004; Diniz et al. 2002; Baker et al. 2009). In this respect, new adsorbents need to be explored during the use of nanotechnologically engineered materials (nanomaterials). Nanomaterials exhibited troop of novel behaviors, such as large surface area, high reactivity, potential for self-assembly, high selectivity, catalytic potential, and the absence of internal diffusion resistance that are promising to improve an existing technology for municipal wastewater treatment (Zhang et al. 2006). Some studies were recently reported in the removal of Pb(II) from water using synthesized nanomaterials, like the application of poly (*N*-isopropylacrylamide) nanoparticles to remove Pb(II) and Cd (II) (Snowden et al. 1993). However, the adsorption capacity for Pb(II) and Cd (II) ions was limited as the ratio of the initiator to *N*-isopropylacrylamide (NIPAm) was kept small in all the synthesis therein. This shortcoming in removal capacity was later surmounted by Morris et al. (1997) by synthesizing it together with a comonomer, as acrylic acid. In addition, the unmodified form of polystyrene nanoparticles do not exhibit any significant heavy metal removal capacity, with a thin shell of poly [(2-acetoacetoxy) ethyl methacrylate] forming core–shell nanoparticles were able to adsorb Co (II), and despite the presence of a 1000-fold excess of other heavy metal ions (Bell et al. 2006). The monomer AMPS is highly hydrophilic polymer that behaves as polyelectrolyte. Separation and enrichment technologies behavior of AMPS emanates from: (1) high water uptake, (2) availability of an active sulfonic group and (3) also having the functional amide group. These actually act as metal ion sorbents (Shoeir et al. 2016a, b; Urbano and Rivas 2012; Chauhan and Garg 2009).

The main objective of this paper, synthesis and characterization of dual temperature and pH-sensitive hydrogels composed of P(AMPS-co-NIPAm) with various molar ratio using methylene-bis-acrylamide (MBA) as crosslinking agent, were prepared by free radical crosslinking copolymerization in aqueous system at 25 °C and crosslinked with (PVA) via (EPC) to form PVA@P(AMPS-co-NIPAm) core–shell nanogels as an adsorbent for preconcentration and determination of trace amount of Pb(II) in water samples. This information will be efficient for further applications of polymeric nanoparticles, particularly in the removal of heavy metal pollutants (Urbano and Rivas 2012).

Materials and methods

Materials

N-Isopropylacrylamide (NIPAm, Across 99% purity) was recrystallized from 1:5 (v:v) toluene and *n*-hexane mixture, 2-acrylamido-2-methyl-1-propane sulfonic acid (AMPS, purchased from Acros), poly(vinyl alcohol) (PVA) (polymerization degree is 1750 + 50, purchased from Acros); *N*,*N*-methylene-bis-acrylamide (MBA), Epichlorohydrin (EPC; Fluka), ammonium peroxydisulfate (APS) was used without further purification, Pb $(NO_3)_2$ of analytical reagent grade obtained from Merck in deionized water. Other reagents were grade and used as received.

Preparation of nanogels sorbent

Shell synthesis

Hydrogel shell particles were synthesized by free radical solution polymerization. In brief, 10 wt% (NIPAm), 90 wt% AMPS (coined AMPS90) and 1% MBA were dissolved in 50 ml of deionized water and the solution was filtered. The solution was heated to 70 °C in a three-neck round-bottom flask. The solution was purged with N_2 gas and stirred until the temperature remained stable for 2 h, and then added dropwise to APS solution (0.5% in 50 ml deionized water) via the semi-batch method at intervals of 2 h. The whole reaction lasted for 4 h under N_2 atmosphere. Similarly, two different (AMPS-co-NIPAm) copolymers hydrogel with 50:50 (%) (Coined AMPS50), and 10:90 (%) (wt.: wt%) (Coined AMPS10), respectively, were synthesized.

PVA nanoparticle core synthesis

2 wt % of PVA was dissolved in 100 ml of distilled water. A solution of 0.66 g NaOH in 5 ml of water was tardily added till pH 12 via syringe with vigorous stirring. After becoming clear and homogeneous, added 15 ml of acetone dropwise with stirring for 30 min. Then, the solution was cooled at 10 °C for 24 h and it became sallow blue, referring that the long chains of PVA shrank to nanoparticles.

Synthesis of PVA@P(AMPS-co-NIPAm) core–shell nanogels

PVA nanoparticle (50 ml) solution was mixed with 1 ml epichlorohydrin and 50 ml of synthesized P(AMPS-co-NIPAm) nanoparticle and heated with stirring at 98 °C for 10 h under N_2 atmosphere to obtain core–shell form. The observed nanogels could be frozen and lyophilized into freeze-dried powder PVA@P(AMPS-co-NIPAm), which can be easily predispersed into the water forming nanoparticle dispersion.

Apparatus and instruments

TEM micrograph analysis of colloidal nanogel particle was taken using a JEOL JEM-2100 electron microscope. AMPS90 nanogel was selected for analysis and prepared

by adding acetone to the aqueous solution till the solution became slightly turbid. The surface area and pore radius determinations were based on isotherms of adsorption–desorption isotherms of N_2 gas at 77 K using Micrometrics gas adsorption analyzer (Nova 3200 USA). The sample was degassed under vacuum at 200 °C for 4 h, using 0.1 g sample for surface area measurements. The thermal stability of the AMPS 90 nanogel was investigated by (TGA) analysis (SDT Q600 V20.5 Build 15) instrument at 20 kV, heating rate of 15 °C/min under nitrogen flow (20 ml/min) starting from room temperature up to 800 °C. The morphology of the nanogels before and after adsorption of Pb(II) was studied using the SEM (S-3400 N II, Hitachi, Japan) operating at an accelerated voltage at 30 kV, the sample was sputter coated with gold prior to evaluate. Metal analysis using the flame atomic absorption spectrophotometer (FAAS) followed the direct aspiration into the air-acetylene flame using the atomic absorption (Hewlett- Packard 3510).

Batch adsorption techniques

To determine the sorption rate of Pb(II), 10 ml containing 100 mg/l of Pb(II) ions were separately prepared with deionized water. Then, 0.05 g AMPS90, AMPS50 and AMPS10 nanogels were added to the solutions. The three solutions were stirred at 25 °C, with an agitation speed of 250 rpm. The concentration of the Pb(II) ions in the aqueous phases at certain times 5–150 min was determined using FAAS. The adsorption percentage and the adsorption uptake q_e were calculated by the following equations:

$$\text{Adsorption}\% = \left(\frac{C_i - C_e}{C_i}\right) \times 100 \quad (1)$$

where, C_i and C_e are the initial and equilibrium concentration of metal ion (mg/l) in the solution. The adsorption uptake was calculated using the mass balance equation for the adsorbent:

$$q_e = \left(\frac{C_i - C_e}{W}\right) \times v \quad (2)$$

where q_e is the amount of Pb(II) adsorption capacity of the nanogels (mg/g), C_i and C_e are the concentrations of Pb(II) in the initial solution and in the aqueous phase after adsorption, respectively (mg/l), V is the volume of the aqueous phase (L) and W is the weight of the nanogels adsorbent (g).

Analytical application

For the analytical performance of the method, three different samples were collected from different sources from the region of Mansoura City, Egypt. The samples were treated with diluted HNO_3 and deionized water, and then filtered through an ashless Whatman 41 filter paper. The samples were stored at 4 °C and the solution pH was adjusted before determination. For adsorptions, 0.05 g portion of the AMPS nanogels and concentrations of 10, 20 and 40 mg/l of the Pb(II) ions were added as spike to 10 ml of the water samples and stirred intermittently for 4 h. The nanogels sorbent were filtered off and dried under vacuum and desorbed in 10 ml 0.1 M HNO_3. The concentration of Pb(II) was detected using FAAS.

Results and discussion

Preparation and characterization of core–shell nanogels

Two approaches for producing PVA@P(AMPS-co-NIPAm) nanogels to enhance colloidal stability and size control were taken. First, a mixture of NIPAm hydrophilic and charged AMPS as a comonomer was added to increase the amount of surface-bound stabilizing moieties. Second, the mixture of AMPS and NIPAm synthesized through free radical solution polymerization and EPC crosslinker were injected semi-continuously to the thermostated reaction containing PVA mixture, the polymerization is typically done around 70 °C above the lower critical solution temperature (LCST) for PNIPAm polymer (~31 °C) that the phase transition of the PNIPAm polymer is entropically favored, such that the rate of polymerization and particle growth manipulated by changing the molar ratio of AMPS and NIPAm monomers addition rate. A multifunctional colloidal stable core–shell nanogel can be achieved by employing SFEP synthesis (Zhang et al. 2009; Shoueir et al. 2016c; Wu et al. 2011). The ionic comonomers, NIPAm and AMPS are responsible for stabilization of nanogels. A possible mechanism of the polymerization of PVA@P(AMPS-co-NIPAm) nanogel is presented in the Scheme 1.

Figure 1, study the SEM surface morphology of AMPS90 nanogel before and after adsorption of Pb(II). The SEM images of AMPS90 nanogel show that adsorbent have a rough surface with non-compact structure. The considerable several pore spaces enable Pb(II) ions to be snared and adsorbed into the pores. Therefore, adsorptive characteristics of AMPS 90 nanogel seems to be highly and more effective. After treatment with Pb(II) ions the pores were adhered and covered by Pb(II).

Figure 2, TEM shows some changes from the initial coil and aggregate caddice-like unattached particulates. A rope-like configuration with aggregates of about 50 nm in diameter indicated that PVA nanoparticles formed well in a mixed solvent of water/acetone (Fouad et al. 2016; Zhang et al. 2007; Yao et al. 2009). Adding of different doses

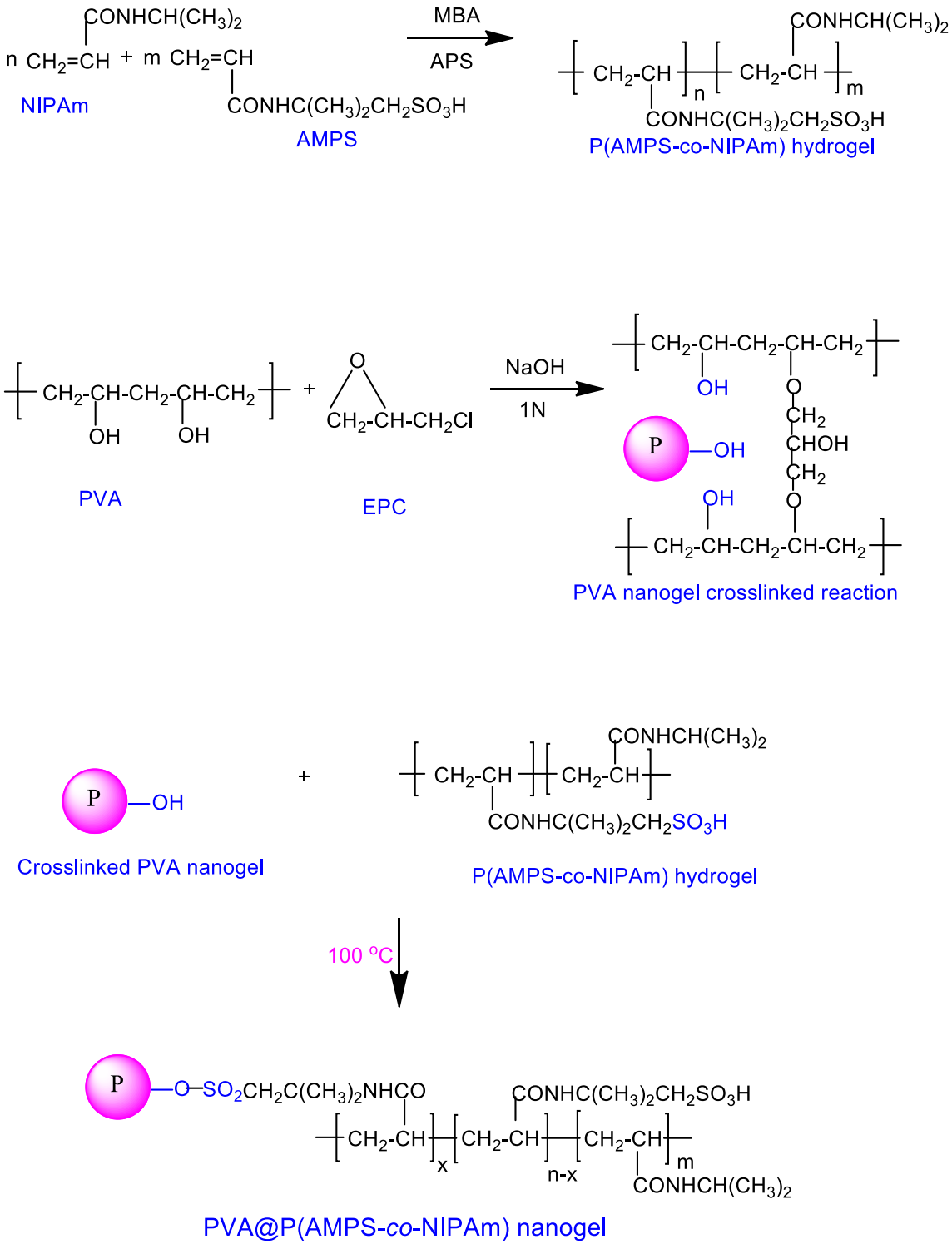

Scheme 1 Synthesis of PVA@P(AMPS-co-NIPAm) nanogels

from P(AMPS-co-NIPAm) to PVA nanogels also investigated. The presence of the hydrophilic PNIPAm may result in distortion of the spherical shape of these particles under dry conditions, and this clearly appeared with increasing PNIPAm content. Insertion of AMPS into the polymerization of NIPAm, coagulation and nucleation were expedited by the hydrogen/bonding interaction between AMPS and NIPAm molecules. Increasing AMPS ratio increased the particle growth throughout the polymerization process to form stable three dimensional

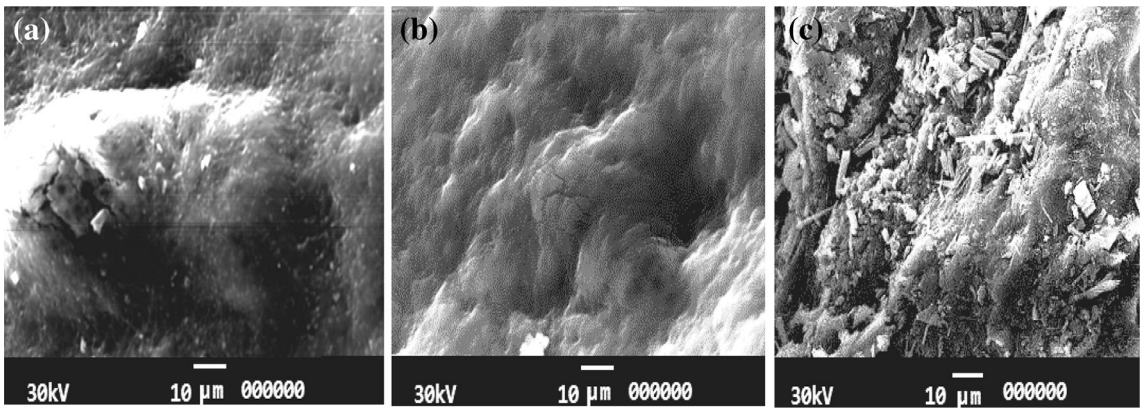

Fig. 1 SEM photograph of AMPS90 nanogel before adsorption with two different views (**a**, **b**) and AMPS90 nanogel adsorbent after treatment with Pb(II) in **c**

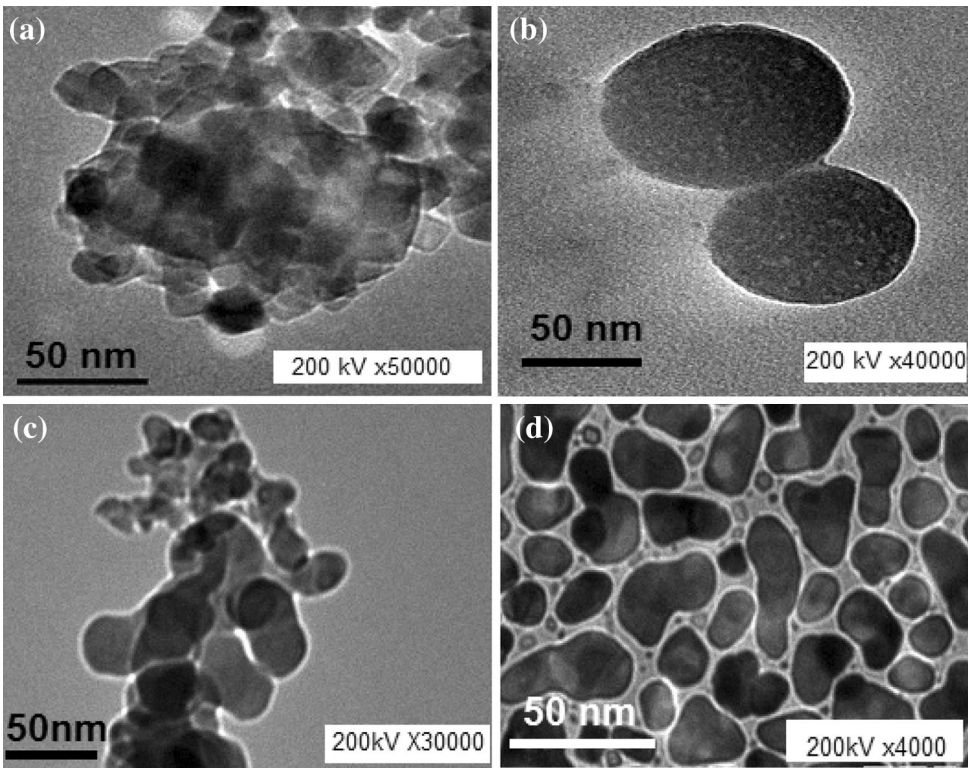

Fig. 2 TEM photograph of PVA@P(AMPS-co-NIPAm) nanogels **a** PVA nanogels in water/acetone cosolvent, **b** AMPS10, **c** AMPS50 and **d** AMPS90 nanogels

network matrix, so that the size of the nanogel networks with high AMPS content were larger than the nanogels contain low AMPS content. As predicted, high content of AMPS90 nanogel provides rigidity to the structure and the ability to adjust the charges in the nano-network.

Figure 3 shows the TGA thermogram of the AMPS90 nanogel. The wt% loss of nanogel shows two steps, the nanogel begins to degrade at 299.73 °C (wt. loss 26.285%) followed by second degradation stage around 519.16 °C. The weight loss around 519.16 °C (17.374 wt%) can emerge from the evaporation of physically absorbed water. It shows that the AMPS90 nanogel has a good thermal stability for adsorption studies.

The nanogel AMPS90 was selected to study the nitrogen adsorption–desorption isotherm. Figure 4 revealed that isotherms take up a shape of the type II isotherm, according to the classification by IUPAC (Sing et al. 1985). Adsorption at a low relative pressure increases steeply, indicating the presence of a large amount of micropores onto AMPS90 nanogel. Isotherms show a small inflection in the region of nearly $p/p^\circ > 0.1$, and at a high relative pressure, $p/p^\circ > 0.8$, where an extent of the adsorption rises rapidly. Such isotherms are characteristic of adsorption on open surfaces with multilayer formation (condensation) occurring in the final stages of the process (Lowell et al. 2004). Figure 4 shows the pore size distribution of

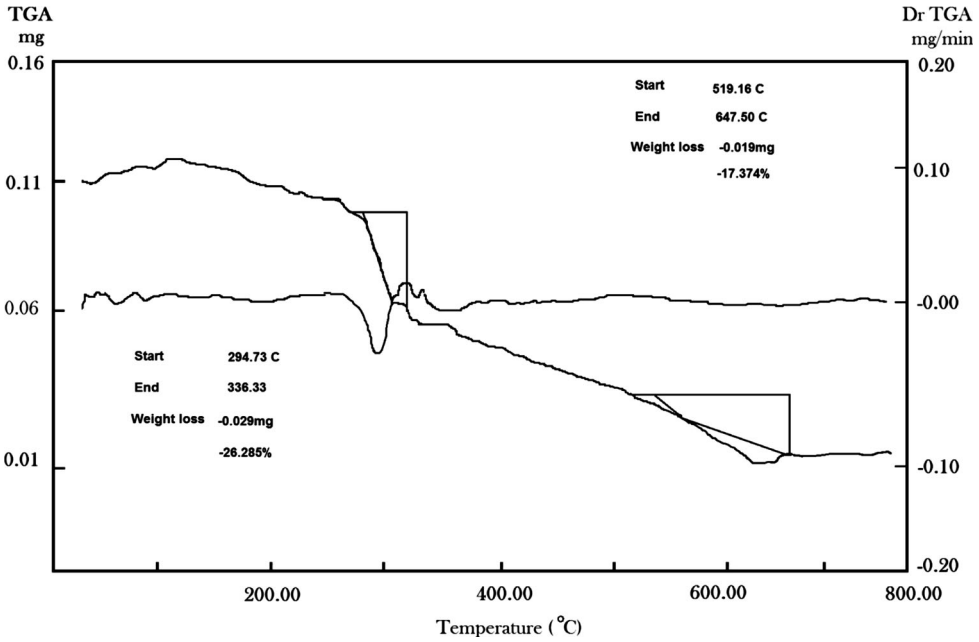

Fig. 3 Thermogravimetric curve of AMPS90 nanogel

AMPS90 nanogel calculated using BJH method. The plot depicted that AMPS90 nanogel concentrated major internal micropore pore radius D$v(r)$ is 1.1603 nm and total pore volume of pores with radius smaller than 224.9 Å at $p/p^{\circ} = 0.955$ is 5.43 cc/g, consistent with the highly specific surface area 1685.808 m^2/g, allows an access of any hydrated metal ions into the interior surface of the AMPS90 nanogel.

Pb(II) adsorption uptake studies

Effect of pH on the adsorption of Pb(II)

The pH sample plays an important role in adsorption performance of the core shell nanogels toward different ions (Wu et al. 2011). Different pH from 1 to 6 was studied, at pH > 5, the Pb(II) ion tends to precipitate as insoluble hydroxides (Khotimchenko et al. 2007). The results were presented in Fig. 5. The reliance of Pb(II) uptake on pH is concerning to the functional groups of the surface of the nanogels adsorbent. At low pH (e.g., pH 2), the –OH, –CONH and $–SO_3H–$ groups in PVA, NIPAm and AMPS, respectively, are protonated, where Pb(II) ions must compete with the H^+ ions for the adsorption sites. At high pH, –OH, –CONH and $–SO_3H$ are ionized, accordingly, the formation of specific interaction with Pb(II) is more favored and Pb(II) adsorbed owing to the negatively charged surface sites of functional groups along the nanogel chain. The removal reached 97.8, 90.8 and 83.7% for AMPS90, AMPS50 and AMPS10 nanogels, respectively. The adsorption of the Pb(II) explained according to the coordination mechanism between Pb(II) and AMPS nanogel (Zhang et al. 2011). The increase in the AMPS content in the nanogel leads to the increment in the ionized sulfonic groups, hence more expansion of the network structure that possesses higher Pb(II) removal. The result shows that the maximum adsorption value of Pb(II) was obtained at pH 5, thus all samples were adjusted to pH 5 as optimum.

Effect of adsorbent dose

The adsorption of Pb(II) was studied by changing the dose of adsorbents (5, 10, 30, 50, 100 and 200 mg/10 ml) in the test solution with keeping the initial concentration 100 mg/l, temperature 25 °C and pH 5 constant for 3 h. The solutions were agitated in a shaker, filtered and the Pb(II) ions concentration in the filtrate was measured. Figure 6 shows that the adsorption of Pb(II) increases quickly with increase in amount of adsorbent and reaches equilibrium after a limit. The maximum removal was obtained at dosage of 50 mg/10 ml for AMPS90, 100 mg/10 ml for AMPS50 and also 100 mg/10 ml for AMPS10 to remove 99, 95 and 92%, respectively. Adding of more doses did not cause any some change in the adsorption sites as a result of serried of adsorbent particles (Brown et al. 2000). Therefore, 0.05 g of AMPS adsorbent was used in all experiments.

Effect of sample volume

The maximum allowed sample volume to determine the high preconcentration factor (P.F) on the adsorption of Pb(II) was also examined. For this purpose, Pb(II) ions were preconcentrated from volumes of 25, 50, 100, 300, 600, 900 and 1000 ml of sample solution containing 10 mg/l Pb(II)

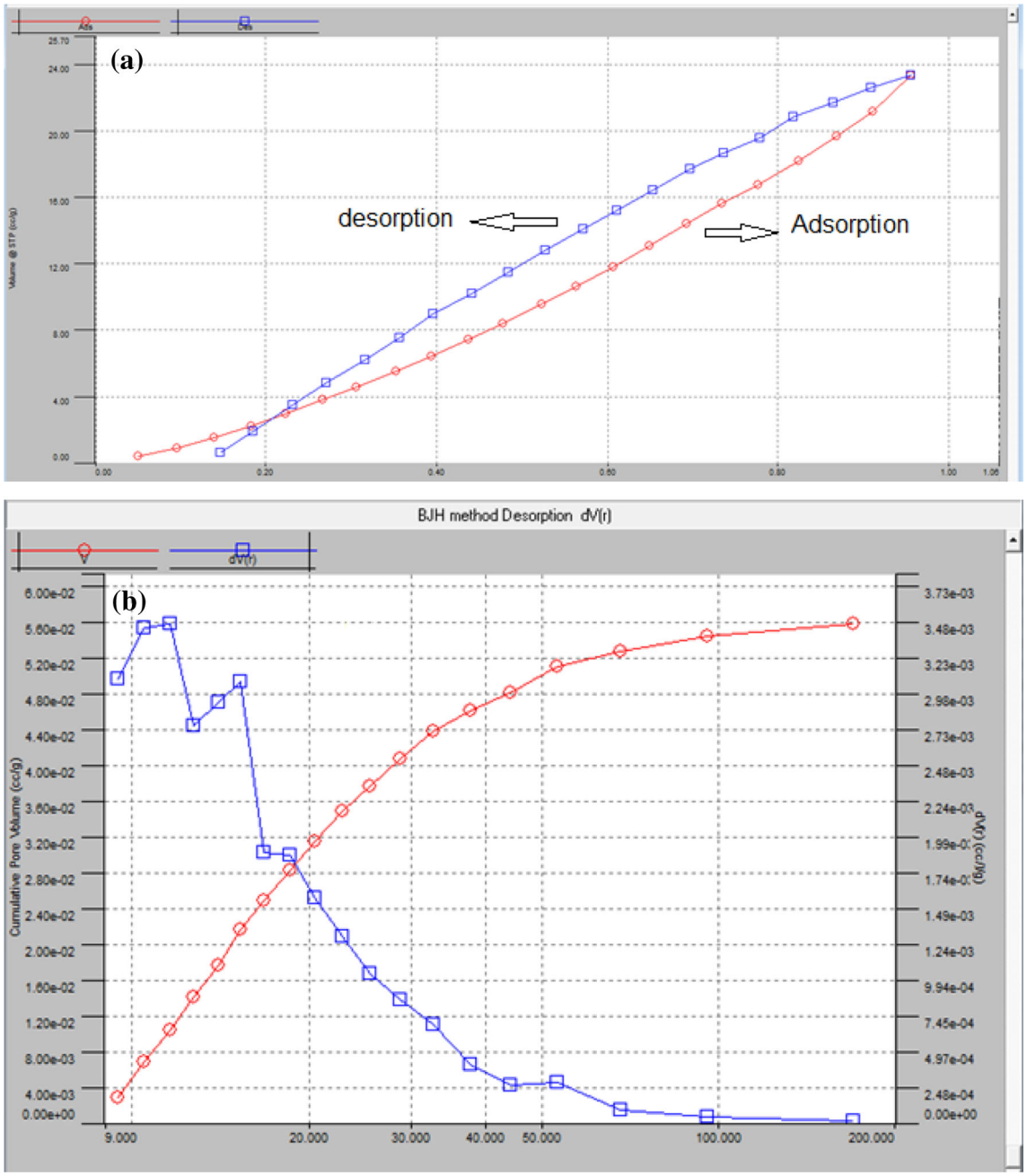

Fig. 4 Nitrogen adsorption isotherm on AMPS90 nanogel at 77 K (**a**), and pore size distribution of AMPS90 nanogel by BJH method desorption d$V(r)$ (**b**)

corresponds to the Pb(II) concentration of 0.4,0.2, 0.1, 0.03, 0.016, 0.011 and 0.01 mg/l Pb(II), respectively. The results are presented in Fig. 7; the recoveries for nanogels are different AMPS90 nanogel is the highest (P.F) 100. High AMPS content in the nanogel structure is primarily responsible for the specific binding of the Pb(II) and the sulfonic acid groups because of the coordination mechanism (Shoueir et al. 2016b; Urbano and Rivas 2012; Fouad et al. 2016; Ayman et al. 2012), and for AMPS50 and AMPS10 (P.F) were 90 and 60, respectively, thus 1000 ml volume were chosen as the largest sample volume to work and the final solution volume to be measured by FAAS was 10 ml. At volumes above 1000 ml probably the analyte ions are not absorbed well onto the nanogels because of low amount of nanogels sorbent in those volumes.

Kinetics of Pb(II) adsorption

Figure 8 shows that the maximum adsorption was found to occur at a time near 50 min for all nanogels. Significantly,

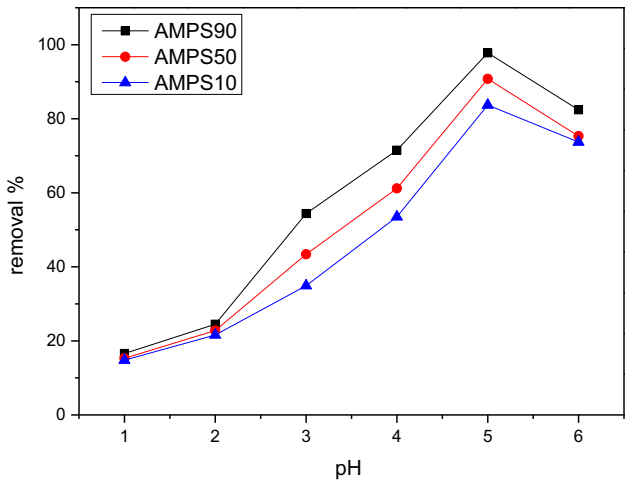

Fig. 5 Effect of pH on the removal percentage (%) of Pb(II) (initial concentration, 100 mg/l; dose, 0.05 g; contact time, 4 h; temperature, 25 °C)

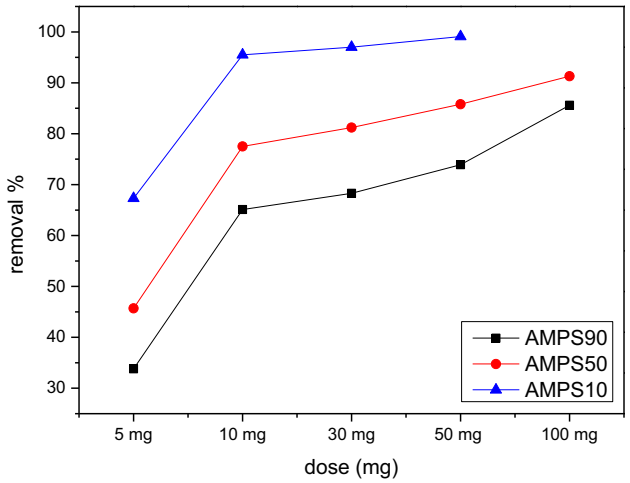

Fig. 6 Removal% of Pb(II) ions at different adsorbent dosage by AMPS nanogels (initial concentration, 100 mg/l; contact time, 3 h; pH, 5; volume, 10 ml; temperature, 25 °C)

more than 98% adsorption was found to occur within AMPS90 nanogel whose underlines the efficiency of the AMPS90 in the removal of toxic materials from waste water. The curve in Fig. 8a was fairly rapid, suggesting formation of monolayer coverage of Pb(II) ions onto nanogels surface. Furthermore, the AMPS90 have high pore volume and excellent BET surface area, which assist the accessibility of sulfonic groups for chelating Pb(II).

The pseudo-first-order and pseudo-second-order kinetic models have been applied to the experimental kinetic data to study the mechanism of Pb(II) adsorption onto nanogels (Ho and McKay 1999; Chen et al. 2011). The pseudo-first-order equation is given as follows:

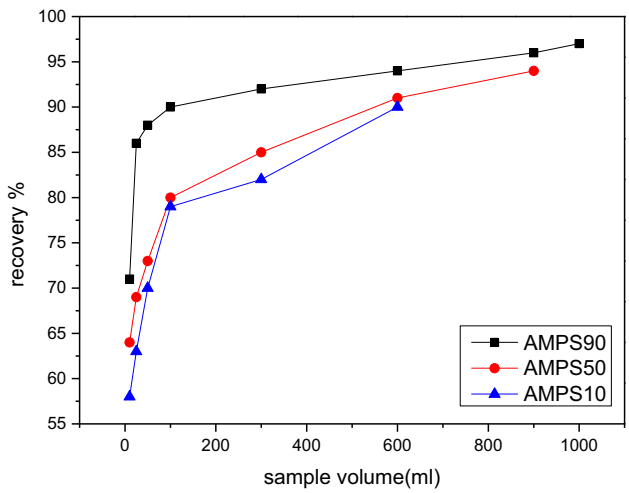

Fig. 7 Effect of sample volume on recovery % by AMPS nanogels (initial concentration, 10 mg/l; contact time, 6 h; pH, 5; temperature, 25 °C)

$$\log(q_e - q_t) = \log q_e - \frac{k_1}{2.303}t \tag{3}$$

where q_e and q_t (mg/g) are the amounts of Pb(II) adsorbed on nanogels adsorbent at equilibrium and at time t, respectively, and k_1 is the pseudo-first-order constant rate (min^{-1}) of adsorption process. Plotting the log ($q_e - q_t$) versus t used to calculate the constant rate k_1 and correlation coefficient R^2. The pseudo-second-order rate expressed as:

$$\frac{t}{q_t} = \frac{1}{k_2 q_e^2} + \frac{t}{q_e} \tag{4}$$

where k_2 is the pseudo-second-order rate constant (g mg^{-1} min^{-1}) of adsorption, R^2 is the correlation coefficient, were determined by plotting the t/q_t versus t. The second kinetic model for Pb(II) adsorption is demonstrated for brevity. The parameter values of the first and second kinetic models are presented in Table 1. The calculated q_e for AMPS90 was (20.8 mg/g) is relatively close to the experimental q_e (19.8) with a high R^2 (0.9987), q_e for the corresponding AMPS50 nanogel was (20 mg/g) and the experimental q_e (18.8 mg/g) with R^2 (0.9964) and q_e for the AMPS10 nanogel was (18.4 mg/g) and the experimental q_e (17 mg/g) estimated from pseudo-second-order kinetic model with R^2 (0.9934). Therefore, the adsorption rate of AMPS90, 50 and 10 nanogels toward Pb(II) were in good correspondence with the pseudo-second-order model. The adsorption mechanism is predominant for the nanogels adsorbent based on the supposal that the rate-limiting step is a chemical sorption.

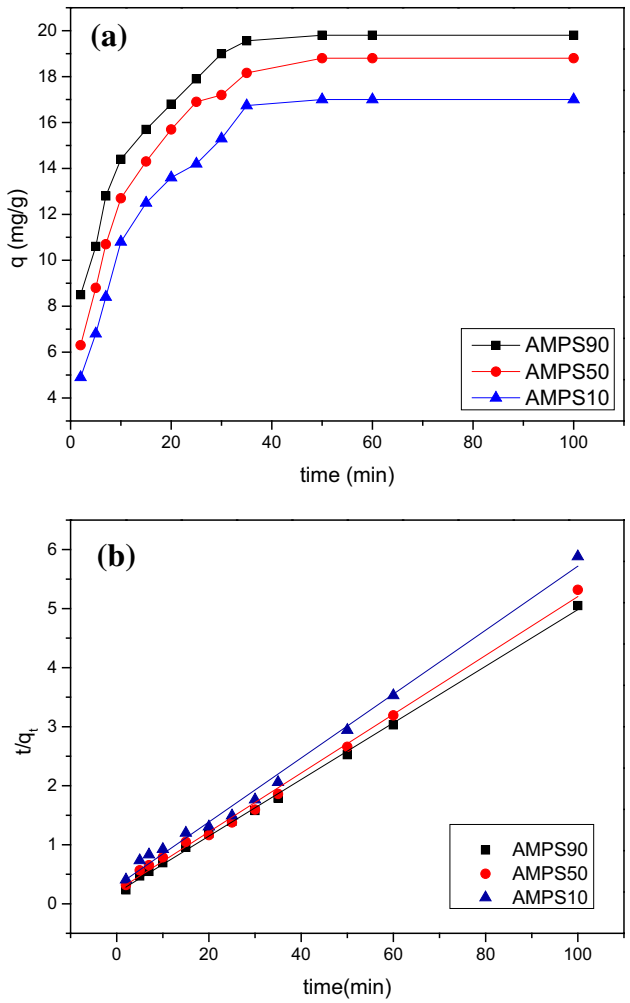

Fig. 8 Effect of time on the uptake of Pb(II) by AMPS nanogels (**a**) and sorption kinetics of the pseudo-second-order model for Pb(II) (**b**) (initial concentration, 100 mg/l; pH, 5; dose, 0.05 g; shaking, 250 rpm; 25 °C

Adsorption isotherm and adsorption capacity

The adsorption capacity of Pb(II) onto AMPS90, 50 and 10 nanogels were determined by the batch technique. Figure 9a shows the adsorption amounts of Pb(II) increased rapidly with increasing initial metal ion concentration from 1 to 500 mg/l, the specific binding sites were not meta-saturated at lower concentration of Pb(II). After an equilibrium level at a maximum concentration of 800 mg/g was reached, indicated that the specific sites of AMPS nanogels were covered with Pb(II) at higher concentrations. The adsorption capacity for AMPS90 (510.2 mg/g), (420.5 mg/g) for AMPS50 and for AMPS10 (329.1 mg/g), suggesting that Pb(II) ions have a stronger attract harmony to the lone pair of electrons in the N,O and S atoms in AMPS90 nanogel to form more stable complexes (Liu et al. 2008).

In this study, Langmuir and Freundlich isotherms were used; the linear form of the Langmuir model is (Brown et al. 2000).

$$\frac{C_e}{q_e} = \frac{1}{k_L q_{\max}} + \frac{C_e}{q_{\max}} \tag{5}$$

where C_e and q_e are the equilibrium concentration of the Pb(II) ions (mg/l) and the equilibrium adsorption capacity (mg/g), respectively. $q_{\max}$ (mg/g) and k_L (mg/l) are Langmuir, $q_{\max}$ and k_L calculated by plotting C_e versus C_e/q_e.

As listed in Table 2, for the two studied systems, the Langmuir and Freundlich isotherms are apposite for characterizing the equilibrium adsorption isotherms since $R^2 > 0.90$, but the Langmuir isotherm yielded R^2 values 0.99 for Pb(II) ions in all AMPS nanogels, the R^2 values for Langmuir isotherm are 0.998, 0.998 and 0.999 for AMPS90, 50 and 10 nanogels, respectively, closest to 1. Hence, it confirms the favorable monolayer adsorption process of Pb(II) onto the AMPS nanogels. The significant increase of the maximum adsorption capacity observed in chelation sites of AMPS90, and interact with Pb(II) ions in complexation yielded efficient surface area resulted from the micropore structure of the AMPS90 wt.(%) at the surface as investigated in SEM section.

Thermodynamic studies

The thermodynamic analysis of Pb(II) adsorption on nanogels adsorbent with experimental data of different temperatures was measured. Thermodynamic parameters like change in free energy ($\Delta G°$, kJ/mol), enthalpy change ($\Delta H°$, kJ/mol) and entropy change ($\Delta S°$, J/K/mol) were calculated using the following equations:

$$\Delta G^\circ = \Delta H^\circ - T\Delta S^\circ \tag{6}$$

Table 1 Kinetic parameters for Pb(II) adsorption onto AMPS nanogels (initial concentration, 100 mg/l; pH, 5; dose, 0.05 g; 25 °C)

Nanogel code	Pseudo-first-order			Pseudo-second-order			
	K_1 (min^{-1})	R_1^2	q_{cal} (mg/g)	K ($gmg^{-1}min^{-1}$)	R_2^2	q_{cal}	q_{exp}
AMPS90	0.1038	0.9381	16.56	0.01234	0.9987	20.8	19.8
AMPS50	0.0829	0.9815	15.03	0.01130	0.9964	20	18.8
MPS10	0.0969	0.8685	16.93	0.00959	0.9934	18.4	17

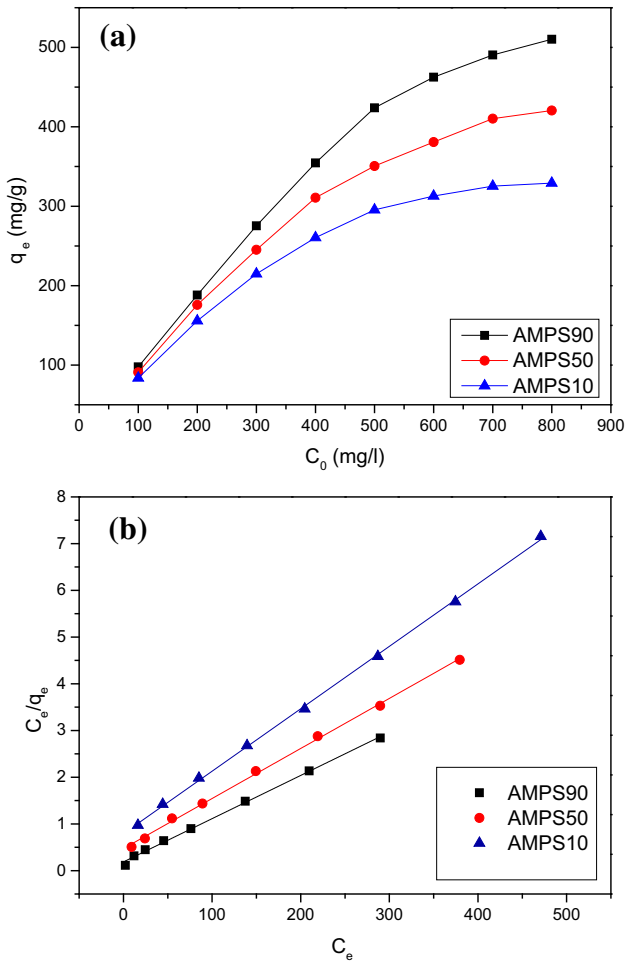

Fig. 9 Effect of initial Pb(II) concentration on adsorption capacity (**a**), fitted Langmuir isotherm (**b**) (initial concentration 100–800 mg/l pH, *5* shaking rate, 250 rpm; dose 0.05 g; 25 °C)

$$\ln b = \Delta S^{\circ}/R - \Delta H^{\circ}/RT \quad (7)$$

The plot of ln b versus $1/T$ according to Eq. (7) was a straight line and the values of ΔH and ΔS were calculated from the slope and intercept of the line. The ΔG calculated using the following equation:

$$\Delta G^{\circ} = -RT \ln b \quad (8)$$

The results of thermodynamic parameters calculated were shown in Table 3. ΔH° is negative in all cases under the same condition of nanogels revealed the exothermic quality of the adsorption of Pb(II). The negative ΔG° indicates the spontaneous behavior of the reaction and the decreasingly negative ΔG° with temperature indicates that the reaction is more favored at lower temperatures. The negative ΔS° reflected the affinity of the nanogels for Pb(II) adsorption, and decrease in the randomness at solid–solution interface during the removal of Pb(II) ions onto AMPS nanogel surfaces, which is widely used in the most of the metal ions uptake process (Yangcheng et al. 2013).

Effect of foreign ions

A certain amount of foreign ion was added to 10 ml of the sample solution containing 100 mg/l of each AMPS90, 50 And 10 nanogels with a pH of 5. Table 4 shows no interference detected of nanogels with ions normally present in natural water, but Cl^- and Ca^{2+} caused serious interference on Pb(II) with AMPS90, 50 and 10 nanogels, formation of soluble chloro complexes at higher concentrations of Cl^- that are responsible for the detected inhibition rate (Karthikeyan et al. 2005). The interference was more in the presence of Ca^{2+} than Cl^- ion at 1000(mg/l), the Ca^{2+} ions being hard acids and form ionic complexes with SO_3H nanogels adsorbent, in addition to Ca^{2+} showed a high positive charge and the ions with smaller hydrated radii decrease the swelling pressure inner the sorbent and increases the affinity of the sorbent for such ions (Kobya et al. 2005). To avoid such high interference, we decrease the concentration to lower value, to obtain low interference.

Environmental applications

Investigating nanomaterial for the removal of any toxins from the real samples from the environment should be considered. The detailed analysis for samples are presented in Table 5; the nanogels able to quantitate the adsorption of Pb(II) ions in all the simulated water samples in the range of 95.7–104.4%. The recoveries (in 40 mg l^{-1}) ranged from 97 to 99.4% for AMPS10 nanogel, 97.1–101.6% for AMPS50 and 97.8–104.4% for AMPS90 for all water samples, indicating that the proposed method of

Table 2 Langmuir and Freundlich isotherm parameters for Pb(II) on AMPS nanogels (initial concentration, 100 mg/l; pH, 5; dose, 0.05 g; 25 °C)

Nanogel code	Langmuir model			Freundlich model			
	K_L (min^{-1})	R_1^2	q_{cal} (mg/g)	q_{exp} (mg/g)	K_F	R_2^2	$1/n$
AMPS90 nanogel	0.0495	0.9980	107.52	102.04	1.03	0.9643	0.34
AMPS50 nanogel	0.0226	0.9987	93.45	84.10	0.785	0.9512	0.39
AMPS10 nanogel	0.0169	0.9995	74.62	65.82	0.169	0.9457	0.40

Table 3 Thermodynamic data for adsorption of Pb(II)

Nanogel code	*b*				−ΔG° (kJ/mol)				ΔH° ads (kJ/mol)	ΔS° (J/mol K)
	298 K	308 K	318 K	328 K	298 K	308 K	318 K	328 K		
AMPS90	44.45	22.04	11.09	5.94	9.38	7.91	6.37	4.85	−54.65	−151.83
AMPS50	9.87	6.02	3.97	2.63	5.67	4.58	3.64	2.64	−35.66	−100.74
AMPS10	5.13	3.11	1.84	1.06	4.06	2.89	1.61	0.16	−42.69	−129.44

Table 4 Interference effect on the recovery % of Pb(II) with AMPS series nanogel

Ion	Conc. (mg/l)	Recovery (%)		
		AMPS90	AMPS50	AMPS10
Na^+ as (NaCl)	1000	97.1	96.7	93.6
K^+ as (KCl)	1000	96.6	93.8	93.9
Ca^{2+}as $Ca(NO_3)_2$	200	87.9	87.4	80.9
	100	91.9	90.1	86.7
	50	95.7	94	90.5
Mg^{2+} as $Mg(NO_3)2Al^{3+}Cl^-$ as NH_4Cl	500	97.8	92.2	91.3
	500	98	95.9	93.1
	500	83.9	80.6	76.4
	200	91.4	88.9	82.7
	50	93.2	91.3	90.2
Br^- as NaBr	100	98.7	93.9	91.7
SO_4^{2-} as Na_2SO_4	1000	98.8	96.7	93.5
CO_3^{2-} as Na_2CO_3	100	94.7	91.9	91
NO_3^- as $NaNO_3$	100	98.4	97.2	92.3

preconcentration and separation procedure could be applied for the determination of Pb(II) ions.

Regeneration of AMPS nanogels is important for potential practical application. For investigation of the reusability and stability of AMPS nanogels, adsorption–desorption cycle was repeated four times using the same nanogels sorbent. The results showed that no hysteresis or loss in adsorption capacity was observed after cycle four and the total amounts of Pb(II) from adsorption and consecutive desorption were in good agreement. Easy removal of Pb(II) ions from the binding sites demonstrated that the AMPS nanogels might be effectively reused several times made it economically suitable for use.

Conclusion

The adsorption behaviors of Pb(II) ions on PVA@-P(AMPS-*co*–NIPAm) nanogels were investigated. It is confirmed that the adsorption of Pb(II) followed the second-order kinetic model and Langmuir isotherm model, affirming that the adsorption mechanism followed Langmuir monolayer adsorption. The chelation occur between

Table 5 Results for Pb(II) determination in various water samples

AMPS nanogels	Recovery (%)			
		Tap Water	Mineral Water	Industrial Effluent
AMPS 90	10	96.5	97.3	99.4
	20	96.8	98.6	101.1
	40	97.8	99.1	104.4
AMPS 50	10	95.8	96.9	98.3
	20	96.6	97.5	99.4
	40	97.1	98.4	101.6
AMPS 10	10	95.7	96.3	97.1
	20	96.4	97	98.5
	40	97	97.9	99.4

the sulfonic groups and Pb(II) ions, excellent surface area depicted that AMPS90 nanogel responsible for such higher adsorption trend, high preconcentration factor, good precision and rapid adsorption rates for the Pb(II) removal. The negative values of $\Delta G°$ and $\Delta H°$ onto AMPS nanogels are spontaneous and endothermic process in nature. No detected interfering of nanogels with ions normally present in natural water. Meanwhile, Cl^- and Ca^{2+} caused severe interference on Pb(II) with AMPS90, 50 and 10 nanogels at concentrations higher than 200 mg/l. AMPS nanogels were successfully applied for determination of Pb(II) at low concentrations in real water samples from different sources. The recovery efficiency was (95.7–104.4) for Pb(II) in the environmental samples under the optimum conditions.

References

Aguado J, Arsuaga JM, Arencibia A, Lindo M, Gascon V (2009) Aqueous heavy metals removal by adsorption on amine-functionalized mesoporous silica. J Hazard Mater 163:213–221

Axtell NR, Sternberg SPK, Claussen K (2003) Lead and nickel removal using microspora and lemna minor. Bioresour Technol 89:41–48

Ayman MA, Hussein SI, Ashraf ME (2012) Application of anionic acrylamide-based hydrogels in the removal of heavy metals from waste water. J Appl Polym Sci 123:2500–2510

Baker HM, Massadeh AM, Younes HA (2009) Nature Jordanian zeolite: removal of heavy metal ions from water sample using column and batch methods. Environ Monit Assess 157:319–330

Bell CA, Smith SV, Whittaker MR, Whittaker AK, Gahan LR, Monterio MJ (2006) Surface-functionalized polymer nanoparticles for selective sequestering of heavy metals. Adv Mater 18:582–586

Brown PA, Gill SA, Allen SJ (2000) Metal removal from wastewater using peat. Water Resour 34:3907–3916

Chauhan GS, Garg G (2009) Study in sorption of Cr^{6+} and NO^{-3} on poly (2-acrylamido-2- methylpropane-1-sulfonic acid) hydrogels. Desalination 239:1–9

Chen CY, Yang CY, Chen AH (2011) Biosorption of Cu(II), Zn(II), Ni(II) and Pb(II) ions by cross-linked metal-imprinted chitosans with epichlorohydrin. J Environ Manage 92:796–802

Darko G, Sobola A, Adewuyi S, Okonkwo JO, Torto N (2012) Preconcentration of toxic metals using electrospun amino-functionalized nylon-6 nanofibre sorbent. S Afr J Chem 65:14–29

Diniz CV, Doyle FM, Ciminelli VST (2002) Effect of pH on the adsorption of selected heavy metal ions from concentrated chloride solutions by the chelating resin dowex M-4195. Sep Sci Technol 37:3169–3185

Fouad RR, Aljohani HA, Shoueir KR (2016) Biocompatible poly (vinyl alcohol) nanoparticle-based binary blends for oil spill control. Mar Pollut Bull 112:46–52

Ho YS, McKay G (1999) Pseudo-second order model for sorption processes. Process Biochem 34:451–456

Ju XJ, Zhang SB, Zhou MY, Xie R, Yang L, Chu LY (2009) Novel heavy metal adsorption material: ion-recognition P(NIPAM-co-BCAm) hydrogels for removal of lead(II) ions. J Hazard Mater 167:114–118

Karthikeyan G, Andal NM, Anbalagan K (2005) Adsorption studies of iron(III) on chitin. J Chem Sci 117:663–672

Khaydarov RR, Gapurova O (2010) Water purification from metal ions using carbon nanoparticle-conjugated polymer nanocomposites. Water Res 44:1927–1933

Khotimchenko M, Kovalev V, Khotimchenko Y (2007) Equilibrium studies of sorption of lead (II) ions by different pectin compounds. J Hazard Mater 149:693–699

Kobya M, Demirbas E, Senturk E, Ince M (2005) Adsorption of heavy metal ions from aqueous solutions by activated carbon prepared from apricot stone. Bioresour Technol 96:1518–1521

Li TT, Liu YG, Peng QQ, Hu XJ, Ting L, Hui W, Ming L (2013) Removal of lead(II) from aqueous solution with ethylenediamine-modified yeast biomass coated with magnetic chitosan microparticles: kinetic and equilibrium modeling. Chem Eng J 214:189–197

Liu YW, Chang XJ, Guo Y, Meng SM (2006) Biosorption and preconcentration of lead and cadmium on waste Chinese herb Pang Da Hai. J Hazard Mater 135:389–394

Liu C, Bai RB, Ly QS (2008) Selective removal of copper and lead ions by diethylenetriamine-functionalized adsorbent: behaviors and mechanisms. Water Res 42:1511–1522

Lowell S, Shields JE, Thomas MA, Thommes M (2004) Characterization of porous solids and powders: surface area, pore size, and density. Academic Press, New York

Mauter MS, Elimelech M (2008) Environmental applications of carbon-based nano-materials. Environ Sci Technol 42:5843–5859

Morris GE, Vincent B, Snowden MJ (1997) Adsorption of lead ions onto *N*-isopropylacrylamide and acrylic acid copolymer microgels. J Colloid Interface Sci 190:198–205

Rao GP, Lu C, Su F (2007) Sorption of divalent metal ions from aqueous solution by carbon nanotubes: a review. Sep Purif Technol 58:224–231

Savage N, Diallo MS (2005) Nanomaterials and water purification: opportunities and challenges. J Nanopart Res 7:331–342

Sekar M, Sakthi V, Rengaraj S (2004) Kinetics equilibrium adsorption study of lead (II) onto activated carbon prepared from coconut shell. J Colloid Interface Sci 279:307–313

Shoueir KR, Sarhan AA, Atta AM, Akl MA (2016a) Macrogel and nanogel networks based on crosslinked poly (vinyl alcohol) for adsorption of methylene blue from aqua system. Environ Nanotech Monit Manage 5:62–73

Shoueir KR, Atta AM, Sarhan AA, Akl MA (2016b) Synthesis of monodisperse core shell PVA@ P(AMPS-co-NIPAm) nanogels structured for pre-concentration of Fe(III) ions. Environ Technol 1–12. doi:10.1080/09593330.2016.1215351

Shoueir KR, Sarhan AA, Atta AM, Akl MA (2016c) Adsorption Studies of Cu^{2+} onto Poly (vinyl alcohol)/Poly (acrylamide-co-*N*-isopropylacrylamide) core-shell nanogels synthesized through surfactant-free emulsion polymerization. Sep Sci Technol. doi:10.1080/01496395.2016.1171237

Sing KSW, Everett DH, Haul RAW, Moscou L, Pierotti RA, Rouquerol J, Siemieniewska T (1985) Pure Appl Chem 57:603

Snowden MJ, Thomas D, Vincent B (1993) Use of colloidal microgels for the absorption of heavy metal and other ions from aqueous solution. Analyst 118:1367–1369

Urbano BF, Rivas BL (2012) Synthesis, characterization, and sorption properties of water-insoluble poly(2-acrylamido-2-methyl-1-propane sulfonic acid)–montmorillonite composite. Polym Bull 18:1–20

Wu AH, Jia J, Luan SJ (2011) Amphiphilic PMMA/PEI core-shell nanoparticles as polymeric adsorbents to remove heavy metal pollutants. Colloids Surf A 384:180–185

Yangcheng L, Jing H, Guangsheng L (2013) An improved synthesis of chitosan bead for Pb(II) adsorption. Chem Eng J 226:271–278

Yao RS, You QD, Liu PJ, Xu YF (2009) Synthesis and pH-induced phase transition behavior of PAA/PVA nanogels in aqueous media. J Appl Polym Sci 111:358–362

Yildi U, Kemika OF, Hazerb B (2010) The removal of heavy metal ions from aqueous solutions by novel pH-sensitive hydrogels. J Hazard Mater 183:521–532

Zhang SN, Cheng FY, Tao ZL, Gao F, Chen J (2006) Removal of nickel ions from wastewater by $Mg(OH)_2$/MgO nanostructures embedded in Al_2O_3 membranes. J Alloy Compd 426:281–285

Zhang L, Guo R, Yang M, Jiang X, Liu B (2007) Thermo and pH dual-responsive nanoparticles for anti-cancer drug delivery. Adv Mater 19:2988–2992

Zhang Q, Zha L, Ma J, Liang B (2009) A novel route to prepare pH- and temperature-sensitive nanogels via a semibatch process. J Colloid Interface Sci 330:330–336

Zhang M, Zhang Z, Liu Y, Yang X, Luo L, Chen J, Yao S (2011) Preparation of core–shell magnetic ion-imprinted polymer for selective extraction of Pb(II) from environmental samples. Chem Eng J 178:443–450